

LHC Tests of Light Neutralino Dark Matter without Light Sfermions

Lorenzo Calibbi ^{*} ¹, Jonas M. Lindert [†] ², Toshihiko Ota [‡] ³, Yasutaka Takanishi ^{*} ⁴

^{*} *Service de Physique Théorique, Université Libre de Bruxelles,
Bld du Triomphe, CP225, B-1050 Brussels, Belgium*

[†] *Physik-Institut, Universität Zürich,
Wintherturerstrasse 190, CH-8057 Zürich, Switzerland*

[‡] *Department of Physics, Saitama University,
Shimo-Okubo 255, 338-8570 Saitama-Sakura, Japan*

^{*} *Max-Planck-Institut für Kernphysik,
Saupfercheckweg 1, D-69117 Heidelberg, Germany*

Abstract

We address the question how light the lightest MSSM neutralino can be as dark matter candidate in a scenario where all supersymmetric scalar particles are heavy. The hypothesis that the neutralino accounts for the observed dark matter density sets strong requirements on the supersymmetric spectrum, thus providing an handle for collider tests. In particular for a lightest neutralino below 100 GeV the relic density constraint translates into an upper bound on the Higgsino mass parameter μ in case all supersymmetric scalar particles are heavy. One can define a simplified model that highlights only the necessary features of the spectrum and their observable consequences at the LHC. Reinterpreting recent searches at the LHC we derive limits on the mass of the lightest neutralino that, in many cases, prove to be more constraining than dark matter experiments themselves.

¹E-mail: lcalibbi@ulb.ac.be

²E-mail: lindert@physik.uzh.ch

³E-mail: toshi@mppmu.mpg.de

⁴E-mail: yasutaka@mpi-hd.mpg.de

1 Introduction

Employing the data collected at 7 and 8 TeV of center of mass energy, the LHC experiments have recently published the results of an impressive number of searches for electroweak production of new physics. In many cases, they were able to set constraints on the masses of new electroweakly-interacting particles above the previous best bounds from LEP. This is the case in particular for the electroweak sector of the minimal supersymmetric standard model (MSSM), as well as of any of its extensions. The exact bounds depend on the details of the spectrum, especially on the mass hierarchy controlling the decay chains, and there is a generic loss of sensitivity in the regime of low mass splittings. However, it is remarkable that, in the most favourable cases, the limits in the MSSM are up to 300 GeV for the sleptons [1, 2] and up to 700 GeV for the charginos and neutralinos [2, 3].

The above mentioned searches have a crucial role in testing supersymmetric Dark Matter (DM) scenarios as they allow to probe the relevant parameter space independently of the colored sector of the theory, which might in principle be too heavy to be directly accessed by the LHC experiments. The cardinal idea is the following: the measurements of the DM relic density based on Cosmic Microwave Background (CMB) observations set non-trivial requirements on the supersymmetric spectrum, thus providing an handle for collider tests. This is true in particular if the lightest supersymmetric particle (LSP) is a bino-like neutralino, whose weak interactions typically lead to overproduction in the early universe, unless an efficient annihilation mechanism is at work. Since a limited set of supersymmetric particles and parameters is involved in the computation of the neutralino annihilation cross section, and hence of its relic density, one can define simplified models that highlight only the necessary features of the spectrum and their observable consequences at the LHC.

The above sketched procedure has been recently employed by us to answer the question on how light the MSSM neutralino is still allowed to be by direct searches for electroweakly-interacting supersymmetric particles at the LHC [4, 5]. Other related studies on light neutralino Dark Matter have been recently published in [6, 7, 8]. For neutralinos lighter than about 30 GeV, the typical spectrum selected by the relic density constraints features rather light staus and Higgsinos, with masses smaller than few hundred GeV [9]. The electroweak production of these particles and the following decays lead to events with multiple taus and missing transverse momentum. Employing an ATLAS search for such a signature in combination with the limits on the decay rate of the Higgs into neutralinos, we could set a lower bound on the DM mass at about 24 GeV. Remarkably, with the above exercise, we showed that electroweak LHC searches are at the moment more powerful than direct and indirect searches in testing light neutralino Dark Matter. For early works addressing limits on light neutralino Dark Matter, see e.g. [10, 11, 12], and for limits on (very) light neutralinos without cosmological bounds we refer to Refs. [13, 14] and references therein.

In the present paper, we want to extend our previous work to the case where no light sfermions are in the spectrum, i.e. scenarios with only neutralinos and charginos lighter than few hundreds GeV. A motivation for such an exercise is that light Higgsinos are the minimal ‘tree-level’ requirement posed by naturalness arguments. A Higgsino-like LSP can not however

account for the full amount of the observed Dark Matter, unless its mass is in the TeV range, since the Higgsino-Higgsino annihilation processes are too efficient, see e.g. [15]. Simultaneous presence of light bino and Higgsinos is thus the minimal ingredient for electroweak scale neutralino Dark Matter in natural SUSY. Scenarios with mixed bino-Higgsino Dark Matter, labelled as ‘well-tempered neutralino’, can provide a natural DM candidate overcoming the above mentioned problems of a pure Higgsino (or wino) LSP [16].¹ We are however interested to focus on the light DM regime (i.e. $m_{\tilde{\chi}_1^0} \lesssim 100$ GeV), where the neutralino can not be ‘well-tempered’ as it is bounded to be mainly bino due to chargino mass limits. Let us note in passing that, even giving up naturalness like in split SUSY scenarios [18, 19], or rather ‘mini-split’ [20] as suggested by the observed Higgs mass, the set-up we are studying is relevant to obtain the absolute lower bound on DM mass. In fact, in these models there are no light sfermions that can mediate the neutralino annihilation and the relic density requirements must fulfilled by the gaugino-Higgsino sector alone.

As we are going to see, possible resonant enhancements of the neutralino annihilation cross section due to s-channel Z and h exchanges play a crucial role in the low mass regime we are going to study. This provides a further, purely phenomenological, motivation for our study: the effective coupling with nuclei for neutralino Dark Matter close to the above mentioned resonances might drastically drop, as well as the today annihilation rate relevant for indirect DM searches, hence one has to find alternative handles to test this corner of the parameter space. As we are going to show, if nature has chosen this peculiar scenario, LHC experiments compete and in some cases prove to be more constraining than dedicated DM experiments.

LHC limits and prospects for the gaugino-Higgsino sector of the MSSM have been recently discussed – however, without a focus on light neutralino DM – in [21, 22, 23, 24, 25, 26, 27], including the challenging case of compressed spectra.

The rest of the paper is organized as follows. In section 2 we present the light neutralino parameter space, where resonant annihilation dominates, including relevant collider and astrophysical constraints. In section 3 we discuss the resulting LHC phenomenology and in section 4 we present the corresponding limits. Finally, in section 5 we conclude.

2 Resonant Neutralino annihilations

As anticipated in the introduction, we are interested to study the phenomenology of the MSSM neutralino as a Dark Matter candidate in the low-mass regime, i.e. with $m_{\tilde{\chi}_1^0} \lesssim 100$ GeV, in the case that only neutralinos and charginos are possibly light, while the rest of the spectrum, in particular the sfermions, might be decoupled. This setup is completely defined by the parameters that describe the gaugino-Higgsino sector in the MSSM:

$$M_1, \quad M_2, \quad \mu, \quad \tan \beta, \tag{1}$$

which are respectively the SUSY-breaking bino and wino masses, the superpotential Higgs mixing parameter that controls the spontaneous electroweak symmetry breaking and sets the

¹For a recent discussion of the LHC prospects of this scenario, see [17].

mass of the Higgsinos, and the ratio of the two Higgs doublets vevs.

As a result of the LEP limit on charginos, $m_{\tilde{\chi}_1^\pm} \approx \min(M_2, |\mu|) \gtrsim 100$ GeV, the lightest neutralino has to be mainly bino in the mass range we consider. As usual, an efficient annihilation mechanism is thus required in order to satisfy the relic density constraints from CMB observations. Since we are assuming that there are no sfermions (and no extra Higgs bosons) below few hundreds GeV or more, the main annihilation modes go through an s -channel Z or h exchange:

$$\tilde{\chi}_1^0 \tilde{\chi}_1^0 \rightarrow Z^*/h^* \rightarrow f\bar{f} \quad (2)$$

Full expressions for the corresponding annihilation cross sections can be found in [28]. Let us recall here that the s -wave contribution vanishes in the h mediation case and it is suppressed by a factor m_f^2/m_Z^2 for a Z exchange. On the other hand, p -wave contributions are in both cases only suppressed by the temperature, $\sim T/m_{\tilde{\chi}_1^0}$, and are therefore relevant for the calculation of annihilation rate in the early universe.

In order to have a qualitative understanding of the dependence of the relic density on the parameters shown in Eq. (1), we have to consider the interactions of the neutralinos with Z and h only. They are given by the following expressions [29]:

$$\mathcal{L}_{\tilde{\chi}_i^0 \tilde{\chi}_j^0 Z} = \frac{g}{2c_W} Z_\rho \tilde{\chi}_i^0 \gamma^\rho [O_{ij}^{ZL} P_L + O_{ij}^{ZR} P_R] \tilde{\chi}_j^0, \quad (3)$$

$$\mathcal{L}_{\tilde{\chi}_i^0 \tilde{\chi}_j^0 h} = \frac{g}{2} C_{ij}^h h \tilde{\chi}_i^0 \tilde{\chi}_j^0, \quad (4)$$

where the couplings are defined as:

$$O_{ij}^{ZL} = -\frac{1}{2} N_{i3} N_{j3}^* + \frac{1}{2} N_{i4} N_{j4}^*, \quad O_{ij}^{ZR} = -O_{ij}^{ZL*} \quad (5)$$

$$C_{ij}^h = \frac{1}{2} [(N_{i2} - N_{i1} \tan \theta_W)(\sin \alpha N_{j3} + \cos \alpha N_{j4}) + (i \leftrightarrow j)]. \quad (6)$$

The matrix N diagonalizes the neutralino mass matrix:

$$\tilde{\chi}_i^0 = N_{i1} \tilde{B} + N_{i2} \tilde{W}^0 + N_{i3} \tilde{H}_d^0 + N_{i4} \tilde{H}_u^0. \quad (7)$$

We refer to the appendix for further details on our conventions and relevant approximate formulae for the elements $N_{i\alpha}$.

From the expressions in Eqs. (3-6), we see that the couplings of the lightest neutralino to Z and h vanish if $\tilde{\chi}_1^0$ is pure bino (or wino), i.e. if $N_{13} = N_{14} = 0$. This only occurs when the Higgsino sector is decoupled, $\mu \gg M_1, m_Z$. In fact, using the approximate expressions shown in the appendix for the Higgsino components of $\tilde{\chi}_1^0$, we find:

$$N_{13} = \frac{m_Z s_W}{\mu} \left[s_\beta + c_\beta \frac{M_1}{\mu} \right], \quad N_{14} = -\frac{m_Z s_W}{\mu} \left[c_\beta + s_\beta \frac{M_1}{\mu} \right], \quad (8)$$

where for simplicity we assumed $M_2 \gg |\mu|$. Here we defined $c_\beta \equiv \cos \beta$, $s_\beta \equiv \sin \beta$ and $s_W \equiv \sin \theta_W$. It is therefore clear that the upper limit on the DM relic density will translate into an upper limit on $|\mu|$, i.e. on the mass scale of the Higgsinos. Thus, relatively light

Higgsinos are a generic prediction of our setup, while from Eqs. (5, 6) it is clear that the wino plays no crucial role in the annihilation process and might in principle be heavier.

A closer look at the expressions for the annihilation cross section reported in [28] shows the well-known possibility of a resonant enhancement of the p -wave annihilation, occurring if

$$m_{\tilde{\chi}_1^0} \approx m_Z/2 \quad \text{or} \quad m_{\tilde{\chi}_1^0} \approx m_h/2. \quad (9)$$

Obviously, the closer $m_{\tilde{\chi}_1^0}$ approaches these conditions the looser the upper bound on μ becomes, since the enhancement can compensate smaller couplings of $\tilde{\chi}_1^0 \tilde{\chi}_1^0 Z$, $\tilde{\chi}_1^0 \tilde{\chi}_1^0 h$. On the other hand, we expect the relic density constraints to set a tighter bound on μ as the mass $m_{\tilde{\chi}_1^0}$ lies further from the resonant conditions of Eq. (9). In what follows, we illustrate and quantify these simple features by means of a numerical scan of the relevant parameters (in section 2.1) and we discuss the LHC phenomenology of this region of resonant neutralino dark matter (in section 3) and the constraints set by searches for chargino-neutralino production (in section 4).

Before moving on, let us comment about the possible role of the extra Higgses. It is well known, that an s -channel exchange of the CP-odd Higgs A can also provide an efficient annihilation mechanism for neutralino DM, especially close to the resonant condition $m_{\tilde{\chi}_1^0} \approx m_A/2$ and/or for a sizeable Higgsino component in $\tilde{\chi}_1^0$ [30]. However, in the light neutralino regime we are considering, A would be required to be relatively light [12, 31, 32, 33]. This possibility is challenged [34] by direct searches for extra Higgses at the LHC [35], as well as by the measurements of the Higgs production and decays, that prove to be SM-like at least at the 30% level (see e.g. [36]), and by rare decays such as $B_s \rightarrow \mu^+ \mu^-$ [37]. For these reasons, here we do not consider the possibility that the extended Higgs sector of the MSSM plays a role in the neutralino annihilation and we assume for simplicity that the heavy Higgses are also decoupled.

2.1 Constraints and viable parameter space

Here we present the results of a random scan of our four parameters within the following ranges:

$$\begin{aligned} 20 \text{ GeV} &\leq M_1 \leq 80 \text{ GeV}, \quad 100 \text{ GeV} \leq M_2 \leq 1 \text{ TeV}, \\ 100 \text{ GeV} &\leq |\mu| \leq 1 \text{ TeV}, \quad 5 \leq \tan \beta \leq 50. \end{aligned} \quad (10)$$

Notice that we scan both signs of μ while we take $M_i > 0$ with no loss of generality: observable effects depend in fact on the relative sign $\text{sgn}(\mu M_i)$. Furthermore we vary the soft parameters of the stop sector in the following ranges:

$$2 \text{ TeV} < m_{\tilde{t}_L}, m_{\tilde{t}_R} \leq 5 \text{ TeV GeV}, \quad -4 \text{ TeV} \leq A_t < 4 \text{ TeV}. \quad (11)$$

Together with the ones in Eq. (10) these parameters determine the value of the physical Higgs mass m_h and thus of the position of the resonance in Eq. (9). The other SUSY soft parameters were set to the following constant values:

$$m_{\tilde{f}} = M_3 = m_A = 4 \text{ TeV}, \quad A_f = 0, \quad (12)$$

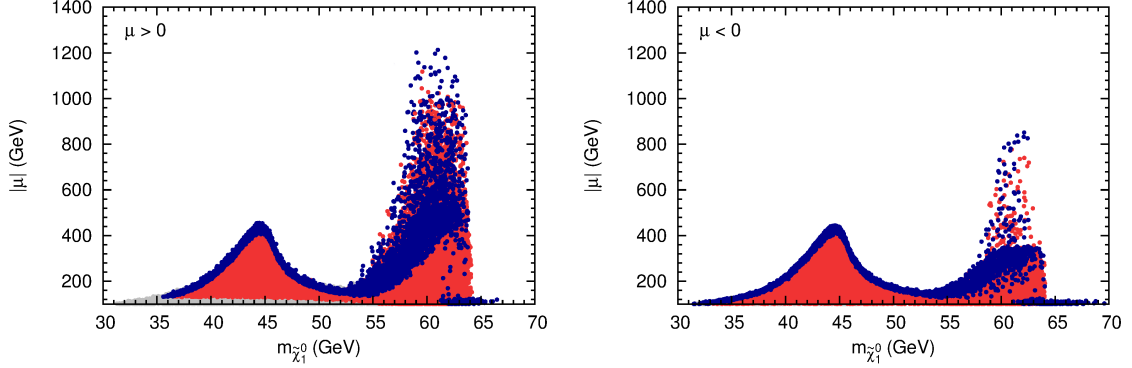


Figure 1: Results of the parameter scan defined in Eqs. (10-12) in the $m_{\tilde{\chi}_1^0} - |\mu|$ plane for $\mu > 0$ (left panel), $\mu < 0$ (right panel). Red points satisfy the relic density upper bound of Eq. (13) and all other constraints discussed in the text. Blue points in addition satisfy the lower bound. Gray points are excluded by one of the constraints listed in the text.

where $m_{\tilde{f}}$ represents the remaining sfermion masses, M_3 is the gluino mass, m_A the CP-odd Higgs mass, A_f the remaining trilinear couplings. The spectrum has been computed by means of the routine **SuSpect** [38], the branching fractions by the **SUSY-HIT** package [39] and **micrOMEGAs** [40, 41, 42, 43] has been used to calculate the neutralino relic density, as well as the scattering cross section with nuclei and the present thermally-averaged annihilation cross section.

The constraints we impose on our parameter space are presented in the following.

- **DM relic density.** We assume a standard thermal history of the universe and take this conservative range from Ref. [44]:

$$0.10 \leq \Omega_{\text{DM}} h^2 \leq 0.13. \quad (13)$$

- **Direct SUSY searches at LEP.** The 95% CL bound on the lightest chargino mass is

$$m_{\tilde{\chi}_1^\pm} \geq 94 \text{ GeV}. \quad (14)$$

Searches for $\tilde{\chi}_1^0 \tilde{\chi}_{2,3}^0$ associated production at LEP, followed by the decay $\tilde{\chi}_{2,3}^0 \rightarrow \tilde{\chi}_1^0 Z^{(*)}$, set a constraint for $m_{\tilde{\chi}_1^0} + m_{\tilde{\chi}_{2,3}^0} \geq \sqrt{s} = 208 \text{ GeV}$. This conservatively reads:

$$\sum_{k=2,3} \sigma(e^+ e^- \rightarrow \tilde{\chi}_1^0 \tilde{\chi}_k^0) \times \text{BR}(\tilde{\chi}_k^0 \rightarrow \tilde{\chi}_1^0 Z^{(*)}) < 100 \text{ fb}. \quad (15)$$

We estimated the production cross sections at LEP using the leading order formulae reported in Refs. [45, 46].

- **Z invisible width.** As discussed above, the relic density constraint require sizeable $\tilde{\chi}_1^0 \tilde{\chi}_1^0 Z$ and $\tilde{\chi}_1^0 \tilde{\chi}_1^0 h$ couplings. As a consequence, the invisible decays $Z \rightarrow \tilde{\chi}_1^0 \tilde{\chi}_1^0$ and

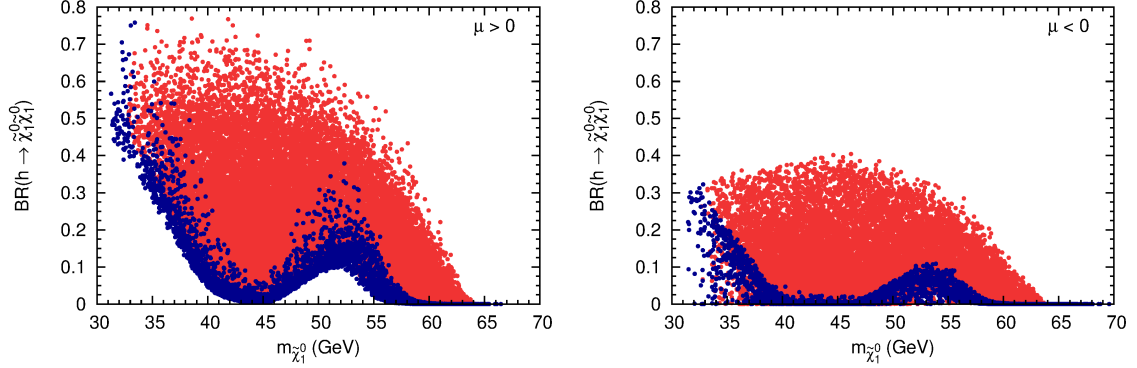


Figure 2: Predictions for the invisible branching ratio of the Higgs $\text{BR}(h \rightarrow \tilde{\chi}_1^0 \tilde{\chi}_1^0)$ in the parameter scan defined in Eqs. (10-12) for $\mu > 0$ (left panel), $\mu < 0$ (right panel). Red points satisfy the relic density upper bound of Eq. (13) and all other constraints discussed in the text. Blue points in addition satisfy the lower bound.

$h \rightarrow \tilde{\chi}_1^0 \tilde{\chi}_1^0$ can occur at relevant rates if kinematically allowed. The decay width of the Z boson into a neutralino pair is given by [47]:

$$\Gamma(Z \rightarrow \tilde{\chi}_1^0 \tilde{\chi}_1^0) = \frac{G_F m_Z^3}{12\sqrt{2}\pi} \left(1 - \frac{4m_{\tilde{\chi}_1^0}^2}{m_Z^2}\right)^{\frac{3}{2}} |N_{13}^2 - N_{14}^2|^2, \quad (16)$$

This has to be compared to the LEP bound on the new physics contribution to $\Gamma(Z \rightarrow \text{invisible})$ [48]:

$$\Delta\Gamma_Z^{\text{inv}} < 3 \text{ MeV} \quad (95\% \text{ CL}). \quad (17)$$

- **Higgs mass and rates.** Applying the tools HiggsBounds [49, 50, 51] and HiggsSignals [52] we calculate a χ^2 measure for the predictions of the model and the measured Higgs rates and mass. We ensure an agreement between the predicted light Higgs mass and production rates and the current experimental measurements at the 95% CL requiring a p-value below 0.002.

- **Invisible Higgs decays.** The light Higgs decay width into $\tilde{\chi}_1^0 \tilde{\chi}_1^0$ is given by [53]:

$$\Gamma(h \rightarrow \tilde{\chi}_1^0 \tilde{\chi}_1^0) = \frac{\sqrt{2}G_F m_W^2 m_h}{\pi} \left(1 - \frac{4m_{\tilde{\chi}_1^0}^2}{m_h^2}\right)^{\frac{3}{2}} |C_{11}^h|^2, \quad (18)$$

where from Eq. (6) one finds in the decoupling regime $m_A \gg m_h$:

$$C_{11}^h = \frac{1}{2} (N_{12} - \tan \theta_W N_{11}) (\sin \beta N_{14} - \cos \beta N_{13}). \quad (19)$$

Since a sizeable $\Gamma(h \rightarrow \text{invisible})$ would reduce by the same amount the branching fractions of all visible channels, it can be constrained by fits to the observed Higgs decay rates. In this work we adopt the limit reported in [36]:

$$\text{BR}(h \rightarrow \text{invisible}) \lesssim 26\% \quad (95\% \text{ CL}). \quad (20)$$

Possible further constraints from electroweak precision observables or the flavour sector can be circumvented adjusting the parameters in Eq. (12).

In Fig. 1 we show the results of the parameter scan in the plane of $m_{\tilde{\chi}_1^0}$ against the Higgsino mass parameter μ for both signs of μ . The red points only fulfill the upper bound of Eq. (13), while the blue ones fulfill the lower bound too. Thus the blue points correspond to models where $\tilde{\chi}_1^0$ can account for 100% of the observed Dark Matter. Points excluded by any of the constraints explained above but the relic density constraint are shown in grey and – marginalizing over all other parameters – they affect the parameter space only for $\mu > 0$ at small values of μ .

As argued already in the previous section, if $m_{\tilde{\chi}_1^0}$ is slightly away from the resonances, Eq. (13) tightly constrains μ . On the other hand, Higgsinos can be as heavy as ≈ 450 GeV close to the Z -pole and as heavy as ≈ 1200 (900) GeV close to the h resonance for $\mu > 0$ ($\mu < 0$). The width and shape of the Higgs resonance is determined by the possible spread in the Higgs mass. Clearly, the parameter region very close to the h resonance is difficult to cover entirely at the LHC.

For illustration in Fig. 2, we explicitly show the invisible branching ratio of the Higgs $\text{BR}(h \rightarrow \tilde{\chi}_1^0 \tilde{\chi}_1^0)$ for both signs of μ obtained in our parameter scan. All constraints but the one from the invisible width of the Higgs itself are applied and the color-coding is as in Fig. 1. As we can see, Eq. (20) excludes points for $m_{\tilde{\chi}_1^0} \lesssim 35$ GeV if $\mu > 0$. For $\mu < 0$ no such limit can be obtained. In fact, as one can see from Eq. (8), a partial cancellation in the $\tilde{\chi}_1^0 \tilde{\chi}_1^0 h$ vertex decreases the coupling if there is a relative sign between μ and M_1 . This is also the reason why smaller values of $|\mu|$ are required close to the h resonance for $\mu < 0$, see Fig. 1. We want to note that for the considered parameter space, regions excluded from the invisible width of the Higgs encompass exclusions from all other constraints considered here.

2.2 Direct and indirect DM searches

As sketched in the introduction, direct and indirect DM searches can loose their sensitivity in the vicinity of the resonant annihilation regimes, Eq. (9). We quantify this behaviour in Fig. 3, where the spin-independent DM-nucleon scattering cross section σ_{SI} (left panel) and the present thermally-averaged annihilation cross section $\langle \sigma_{\text{ann}} v \rangle$ (right panel) are plotted as a function of the lightest neutralino mass for the points of our parameter scan defined in Eqs. (10-12). All shown points account for the observed DM abundance, i.e. they satisfy the upper and lower bound of Eq. (13) besides all other constraints discussed in section 2.1. Red (purple) points correspond to $\mu > 0$ ($\mu < 0$).

In the left panel, we show as a reference the current limit set by the direct search experiment LUX [54], which for the considered mass range is almost independent of the neutralino mass at $\sigma_{\text{SI}} \lesssim 8 \times 10^{-46} \text{ cm}^2$. Close to the resonances the predicted σ_{SI} is suppressed by several orders of magnitude and tests of such scenarios even in future direct DM search experiments seems to be very challenging. The neutralino elastic scattering with nuclei is mediated by the exchange of CP-even Higgs states or squarks (which we assume to be decoupled). Thus, the shown suppression originates from small Higgs-Higgsino-bino couplings, as given in Eq. (6),

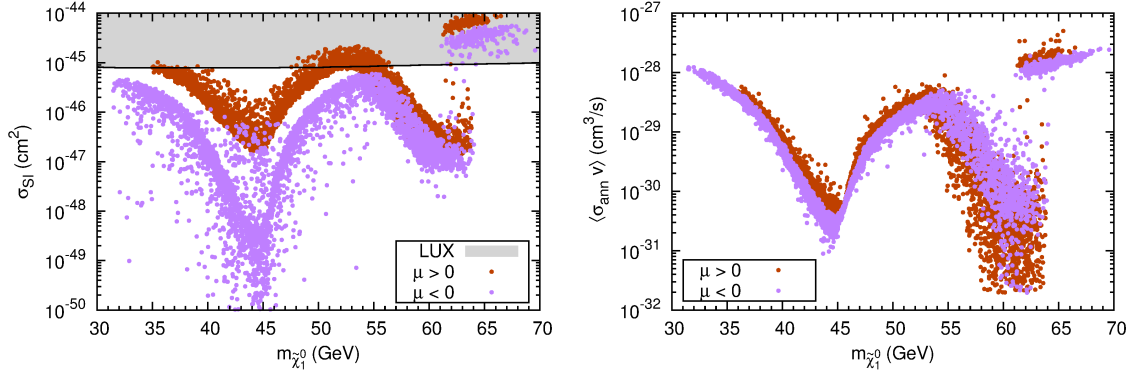


Figure 3: Predictions for the spin-independent DM-nucleon scattering cross section σ_{SI} (left panel) and the present thermally-averaged annihilation cross section $\langle\sigma_{\text{ann}}v\rangle$ (right panel) in the parameter scan defined in Eqs. (10-12). All points satisfy the upper and lower bound of Eq. (13) and all other constraints discussed in section 2.1. The gray shaded area in the left plot is excluded from direct DM searches with LUX.

close to the resonances (due to large μ as required by the relic abundance). Larger values of this coupling, i.e. a smaller μ parameter would reduce the neutralino density $\Omega_{\tilde{\chi}^0}$ below the observed value, which would require extra DM components and, more importantly for us, anyway would reduce the sensitivity of direct detection by a factor $\Omega_{\tilde{\chi}^0}/\Omega_{\text{DM}}^{\text{obs}}$. However, we have to keep in mind that the theoretical prediction for σ_{SI} suffers from large uncertainties: variations of light quark masses and hadronic form factors, as well as heavier values of $m_H \approx m_A$ (here we took $m_A = 4$ TeV) can further reduce the predicted σ_{SI} by a factor of few. On the other hand, lighter heavy Higgs states, i.e. smaller values of m_A could in principle increase the spin-independent cross section without altering much the relic density prediction. Therefore, we refrain from setting any conservative constraints on our parameter space from direct detection.

Similarly to the discussion above, we observe in the right panel of Fig. 3 that the predicted $\langle\sigma_{\text{ann}}v\rangle$ is well below the sensitivity of indirect detection experiments – which are currently at the level of 10^{-26} cm³/s [55] – and further drops in the vicinity of the resonances. The reason why the present $\langle\sigma_{\text{ann}}v\rangle$ is much lower than the value required by a thermal WIMP at the freeze-out can be understood by the following: at high temperatures the annihilation is dominated by resonant p -wave contributions which become irrelevant as the temperature drops. In the present universe, the annihilation occurs through a Z -mediated s -wave amplitude. The corresponding cross section is suppressed by a factor m_f^2/m_Z^2 . Furthermore, as above, close to the resonances a small Higgsino component in $\tilde{\chi}_1^0$ further suppresses the $\tilde{\chi}_1^0\tilde{\chi}_1^0Z$ coupling. Again an additional possible contribution to $\langle\sigma_{\text{ann}}v\rangle$ is expected to be provided by an s -channel exchange of a CP-odd Higgs A . We checked that even for masses at the border of the present LHC exclusion, e.g. $m_A \simeq 500$ GeV for $\tan\beta = 20$ [35], $\langle\sigma_{\text{ann}}v\rangle$ can not increase by more than one order of magnitude with respect to the values shown in Fig. 3.

3 LHC phenomenology

The spectrum we consider solely involves the neutralino/chargino sector of the MSSM. As discussed above, the relic density constraint translates into an upper bound on the Higgsino mass parameter μ , while the wino mass parameter M_2 does hardly play a role satisfying those bounds. Thus, the minimal particle content are just the mostly bino-like neutralino LSP and the Higgsino states: two heavier neutralinos and the lightest charginos. Later we will demonstrate that additional light winos just increase the LHC sensitivity. Hence, taking M_2 to be large is a conservative assumption and will be assumed if not otherwise stated. All other SUSY particles are assumed to be decoupled.

For the described spectrum possible tests at the LHC rely on electroweak Drell-Yan production of the Higgsino-like states:²

$$pp \rightarrow \tilde{\chi}_k^0 \tilde{\chi}_l^0, \quad pp \rightarrow \tilde{\chi}_1^+ \tilde{\chi}_1^-, \quad pp \rightarrow \tilde{\chi}_1^\pm \tilde{\chi}_k^0, \quad (k, l = 2, 3). \quad (21)$$

The produced charginos can only decay into the LSP and (on- or off-shell) W bosons:

$$\tilde{\chi}_1^\pm \rightarrow W^{\pm(*)} \tilde{\chi}_1^0, \quad (22)$$

whereas the neutralinos have two competing decay modes, Z or h :

$$\tilde{\chi}_{2,3}^0 \rightarrow Z^{(*)} \tilde{\chi}_1^0, \quad \tilde{\chi}_{2,3}^0 \rightarrow h^{(*)} \tilde{\chi}_1^0 \quad (23)$$

with relevance depending on the model parameters as discussed in the following.

The most relevant searches for neutralino/chargino production performed by the LHC collaborations are based on leptonic decays of the gauge bosons, i.e. on events with multiple leptons plus missing transverse momentum. For the parameter space we consider by far the highest sensitivity is reached in the WZ -channel [27] (from associated neutralino-chargino production, $\tilde{\chi}_1^\pm \tilde{\chi}_{2,3}^0$) with three reconstructed leptons in the final state [2, 3]. In this channel the search performed by ATLAS [3] sets the most stringent limits. Searches for the Higgs decay have been performed in the Wh -channel with $h \rightarrow b\bar{b}$ [2], see also [23, 58]. The complementary $h \rightarrow \tau^+ \tau^-$ channel might yield a similar sensitivity [59]. However, the overall sensitivity in the Wh -channel is considerably weaker compared to the WZ -channel. Still, it is in order to investigate in detail the rates of the competing decay modes shown in Eq. (23). The decay rates of $\tilde{\chi}_{2,3}^0 \rightarrow Z \tilde{\chi}_1^0$ are controlled by the couplings defined in Eq. (5). Using the approximate expressions for the neutralino mixing in the Higgsino-like $\tilde{\chi}_{2,3}^0$ limit $M_2 \gg |\mu|$, as reported in the appendix Eq. (38), we find:

$$\mu > 0: \quad O_{21}^{ZL} \simeq \frac{m_Z s_W}{2\sqrt{2}\mu} (s_\beta - c_\beta) \left(1 + \frac{M_1}{\mu}\right), \quad O_{31}^{ZL} \simeq \frac{m_Z s_W}{2\sqrt{2}\mu} (s_\beta + c_\beta) \left(1 + \frac{M_1}{\mu}\right); \quad (24)$$

$$\mu < 0: \quad O_{21}^{ZL} \simeq -\frac{m_Z s_W}{2\sqrt{2}\mu} (s_\beta + c_\beta) \left(1 + \frac{M_1}{\mu}\right), \quad O_{31}^{ZL} \simeq \frac{m_Z s_W}{2\sqrt{2}\mu} (c_\beta - s_\beta) \left(1 + \frac{M_1}{\mu}\right), \quad (25)$$

²Monojet searches for direct production of a pair of neutralino LSPs in association with a jet can in principle also test the given spectrum but will only become sensitive in the future [56, 57].

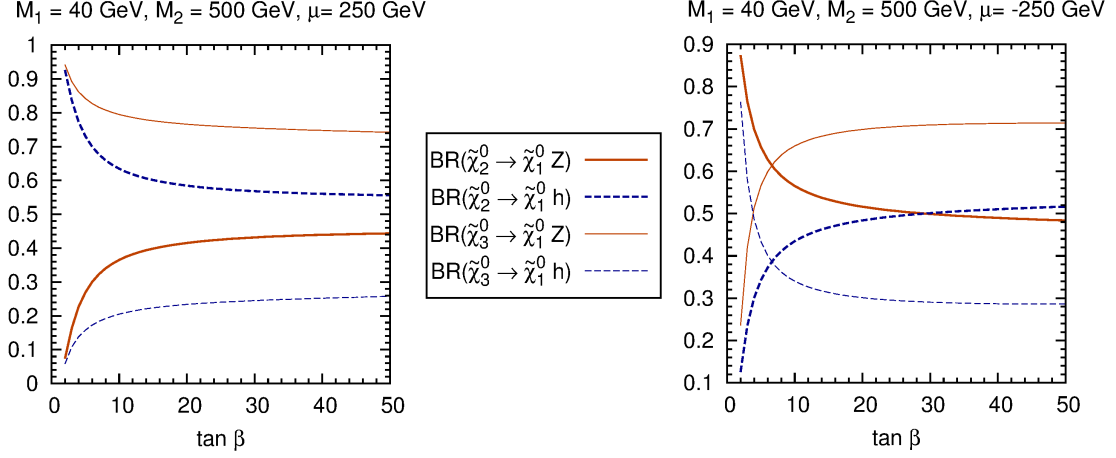


Figure 4: Branching ratios for the decay $\tilde{\chi}_{2,3}^0 \rightarrow \tilde{\chi}_1^0 Z/h$ as function of $\tan \beta$. Parameters are chosen to be $M_1 = 40$ GeV, $M_2 = 500$ GeV and $\mu = \pm 250$ GeV for the left/right plot.

Analogous expressions for the coupling $\tilde{\chi}_{2,3}^0 \tilde{\chi}_1^0 h$ can be obtained from Eqs. (6, 38):

$$\mu > 0 : \quad C_{21}^h \simeq -\frac{1}{2\sqrt{2}}(c_\beta + s_\beta), \quad C_{31}^h \simeq -\frac{1}{2\sqrt{2}}(c_\beta - s_\beta); \quad (26)$$

$$\mu < 0 : \quad C_{21}^h \simeq -\frac{1}{2\sqrt{2}}(c_\beta - s_\beta), \quad C_{31}^h \simeq -\frac{1}{2\sqrt{2}}(c_\beta + s_\beta). \quad (27)$$

From these expressions we expect that for $\mu > 0$ the branching ratio $\text{BR}(\tilde{\chi}_2^0 \rightarrow Z\tilde{\chi}_1^0)$ decreases for small values of $\tan \beta$, and vanishes in the limit $\tan \beta \rightarrow 1$. Whereas the branching ratio $\text{BR}(\tilde{\chi}_3^0 \rightarrow Z\tilde{\chi}_1^0)$ is maximized in the low $\tan \beta$ regime. This behaviour is depicted in the left panel of Fig. 4, where for illustration we choose $M_1 = 40$ GeV, $M_2 = 500$ GeV and $\mu = 250$ GeV. The behaviour described above is reversed for $\mu < 0$, as shown in the right panel of Fig. 4. Clearly, the WZ channel is expected to suffer a loss of sensitivity in the low (large) $\tan \beta$ regime for $\mu > 0$ ($\mu < 0$). However, as the behavior of the two Higgsino-like neutralinos $\tilde{\chi}_{2,3}^0$ is antipodal³ and their mass splitting is in general small, the $\tan \beta$ dependence in the total sensitivity of the WZ channel is moderate. In our numerical analysis in section 4 we consider the two example values $\tan \beta = 5, 40$. Furthermore, as the summed contribution only mildly depend on $\tan \beta$ even for small values of $\tan \beta$ the WZ -channel is expected to remain more sensitive than the Wh -channel.

Searching for neutralino and chargino production in the three leptons plus missing energy final state performed by ATLAS [3] the strongest available limits for the WZ channel have been obtained. These limits have been interpreted in the $M_2 - \mu$ plane of the pMSSM for fixed values of M_1 and in terms of constraints on the mass of purely wino-like charginos and neutralinos with $\text{BR}(\tilde{\chi}_2^0 \rightarrow \tilde{\chi}_1^0 Z) = 100\%$. Clearly, the latter is only a simplified model as for a pure wino-like $\tilde{\chi}_2^0$ state the coupling $\tilde{\chi}_1^0 \tilde{\chi}_2^0 Z$ vanishes. The corresponding limits for a realistic

³Also the production cross sections depend on $\tan \beta$ via the $\tilde{\chi}_{2,3}^0 \tilde{\chi}_1^\pm Z$ couplings. For fixed physical masses the dependence is very mild and again antipodal to the corresponding dependence in the branching ratios.

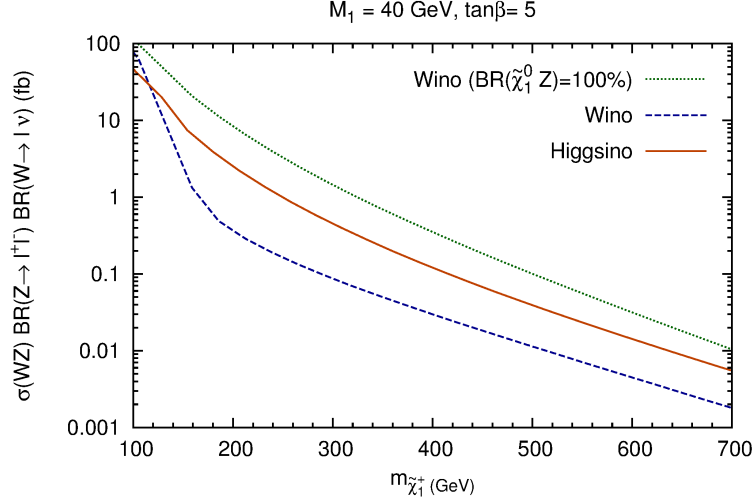


Figure 5: Comparison among the simplified wino model with $\text{BR}(\tilde{\chi}_2^0 \rightarrow Z\tilde{\chi}_1^0)=100\%$, a realistic wino model with $M_2 \ll \mu$ and an Higgsino model with $\mu \ll M_2$. Shown is the summed neutralino-chargino production cross section times branching ratios into $W(\rightarrow \ell^\pm \nu)Z(\rightarrow \ell^+ \ell^-)$ as defined in Eq. (28).

scenario with Higgsino-like neutralinos and charginos might be much weaker due to changes in the cross section and possible competing decay modes as discussed above. Therefore, in section 4 we will reinterpret those limits for Higgsino-like neutralinos in a detailed analysis including detector effects. Here, we already want to anticipate those results qualitatively. To this end we compare the production cross section times branching ratio for the WZ channel defined as

$$\sigma_{3\ell+ \cancel{E}_T} = \sum_{\substack{k=1,2 \\ l=2,3,4}} \sigma(\tilde{\chi}_k^\pm \tilde{\chi}_l^0) \text{BR}(\tilde{\chi}_l^\pm \rightarrow W^\pm \tilde{\chi}_1^0) \text{BR}(\tilde{\chi}_l^0 \rightarrow Z\tilde{\chi}_1^0) \text{BR}(W^\pm \rightarrow \ell^\pm \nu) \text{BR}(Z \rightarrow \ell^+ \ell^-), \quad (28)$$

for the cases of (i) the simplified model, (ii) realistic wino-like $\tilde{\chi}_2^0$ case, and (iii) Higgsino-like $\tilde{\chi}_{2,3}^0$ case. The corresponding estimated rates are shown in Fig. 5 as a function of the mass of $\tilde{\chi}_1^\pm$, where (leading order) production cross sections are calculated with **Prospino 2** [60] and BRs with **SUSY-HIT** [39]. In the Higgsino-like $\tilde{\chi}_{2,3}^0$ case, we set $M_2 = 1$ TeV and, vice versa, we set $\mu = 1$ TeV in the wino-like $\tilde{\chi}_2^0$ cases. For all scenarios we additionally set for illustration $M_1 = 40$ GeV and $\tan\beta = 5$. Clearly, for realistic values of $\text{BR}(\tilde{\chi}_2^0 \rightarrow Z\tilde{\chi}_1^0)$ compared to the simplified model the sensitivity is strongly reduced in the wino-like $\tilde{\chi}_2^0$ case. Resulting rates are here also considerably smaller than in the Higgsino-like $\tilde{\chi}_{2,3}^0$ case – despite the fact that the production cross section for wino states is typically larger than the one for Higgsinos. In [3] ATLAS obtains (approximately) the limit $m_{\tilde{\chi}_1^\pm} \gtrsim 350$ GeV for $m_{\tilde{\chi}_1^0} \lesssim 100$ GeV under the assumption of $\text{BR}(\tilde{\chi}_2^0 \rightarrow Z\tilde{\chi}_1^0)=100\%$. Comparing such a limit in Fig. 5 to the Higgsino-like $\tilde{\chi}_{2,3}^0$ case we expect an exclusion on $m_{\tilde{\chi}_1^\pm} \approx m_{\tilde{\chi}_2^0} \approx m_{\tilde{\chi}_3^0}$ weaker by about

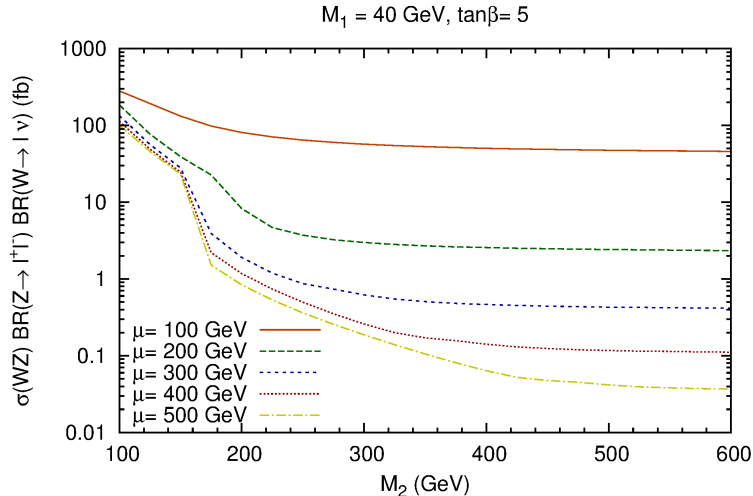


Figure 6: Impact of M_2 on the summed neutralino-chargino production cross section times branching ratios into $W(\rightarrow \ell^\pm \nu)Z(\rightarrow \ell^+ \ell^-)$ as defined in Eq. (28) for different values of μ .

100 GeV. Still, this represents a non-negligible constraint on the neutralino DM parameter space.

Finally, let us turn to a short discussion of the possible impact of the wino mass M_2 on the signal rates in the WZ channel. For $M_2 \lesssim |\mu|$, the full set of neutralinos and charginos contributes to the production cross section, providing additional modes to those shown in Eq. (21). Hence it is natural to expect an increase in sensitivity. This is confirmed and quantified in Fig. 6, where we plot again cross section times branching ratio, as defined in Eq. (28), now as a function of M_2 for different choices of μ . In Fig. 6 we see that the number of expected leptonic events generically increases for low values of M_2 , whereas it becomes approximately flat for $M_2 > \mu$. As a consequence, fixing M_2 at some value larger than μ can be regarded as a conservative choice. We are going to adopt this choice in the numerical simulation of the next section.

Let us note here that further MSSM parameters, besides those of the neutralino/chargino sector, cf. Eq. (1), have in general little impact on the searches based on electroweak production of Higgsinos and their decay. In particular, the production cross sections have no dependence on any squark masses, in contrast to the wino case, for which t -channel squark exchange decouples only very slowly and can be relevant even for very heavy squarks [59]. In contrast to the wino case the Higgsinos have only small couplings with first and second generation quarks and squarks rendering such contributions negligible.

4 LHC limits

As discussed in the last section, the scenario under consideration can best be searched for at the LHC in the WZ channel, where both CMS and ATLAS have performed different searches

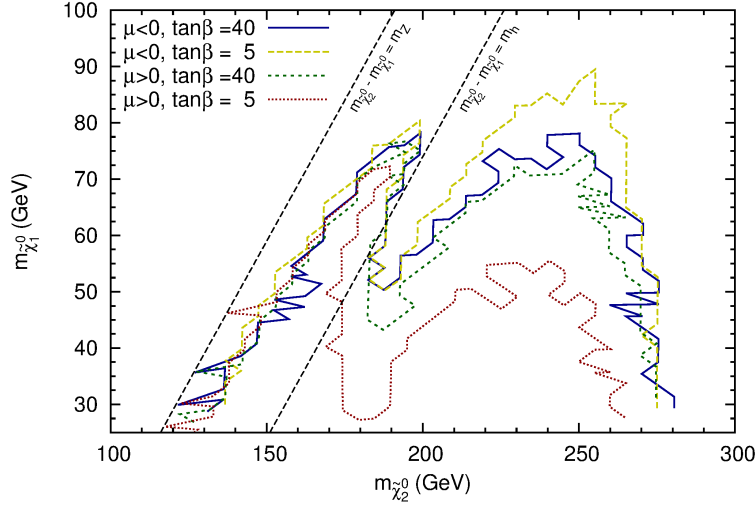


Figure 7: Reinterpreted ATLAS limit [3] for the Higgsino-like $\tilde{\chi}_{2,3}^0$ case, displayed in the $m_{\tilde{\chi}_2^0} - m_{\tilde{\chi}_1^0}$ plane for different values of $\tan\beta$, $\text{sgn}(\mu)$. See the text for details.

using the full dataset available at 8 TeV [1, 2, 3]. The most stringent limit available is deduced from the three-leptons plus missing energy search performed by ATLAS [3]. In the relevant signal region three leptons have to be identified, where two of them have to be of the same flavour and of different sign (SF-OS). The resulting event sample is further divided into 16 bins with different invariant mass cuts for the SF-OS pair, different cuts on the transverse mass m_T and/or different cuts on the transverse missing energy \cancel{E}_T . Final event numbers are found to be in good agreement with Standard Model predictions. Interpreting the resulting limits in a pure wino scenario⁴ with $\text{BR}(\tilde{\chi}_2^0 \rightarrow Z\tilde{\chi}_1^0) = 100\%$ (as explained above) ATLAS sets bounds up to $m_{\tilde{\chi}_1^\pm} = m_{\tilde{\chi}_2^0} \gtrsim 350$ GeV for a massless neutralino. Furthermore, the ATLAS collaboration interprets the search in the $M_2 - \mu$ -plane of a pMSSM scenario with decoupled sfermions, a bino of $M_1 = 50$ GeV and $\tan\beta = 10$. Here, for $M_2 \gg \mu$ a limit of $\mu \gtrsim 230$ GeV is derived. We want to reinterpret this limit in the light neutralino scenario discussed above, where we vary both M_1 and $\tan\beta$ (besides μ and M_2).

In our Monte Carlo study we use **Herwig++** [62] for event simulation and rescale the obtained LO rates with NLO K-factors obtained from **Prospino 2** [60]. Furthermore, we use the powerful **CheckMate** [63] framework for detector simulation (where a tuned version of **Delphes 3** [64] is used internally), analysis and statistical evaluation. First, we carefully verified that the three-leptons plus missing energy analysis implemented in **CheckMate** yields limits for the pure-wino scenario and the pMSSM scenario which are in good agreement with the ones published by ATLAS. Second, we evaluate those limits in the benchmark scenarios motivated in section 3, i.e. we translate the ATLAS limits into the $M_1 - \mu$ plane for $\tan\beta = 5, 40$ and $\mu \gtrless 0$. As discussed in section 3, for $\mu > 0$, $\tan\beta = 5$ gives a conservative limit while $\tan\beta = 40$ gives a limit in the plateau shown in Fig. 4. On the contrary, for $\mu < 0$,

⁴In this scenario the sfermions are decoupled at $m_{\tilde{f}} = 5$ TeV as listed on HepData [61].

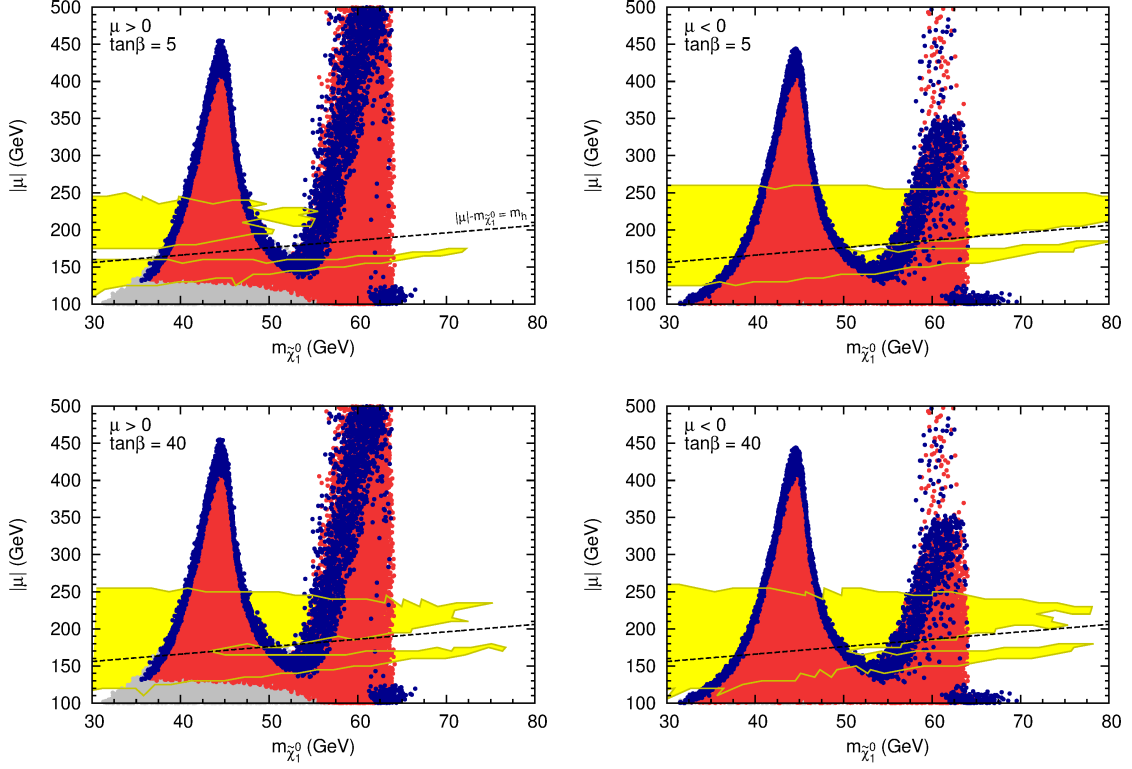


Figure 8: Reinterpreted ATLAS limit, displayed in the $m_{\tilde{\chi}_1^0} - |\mu|$ plane of Fig. 1 for different values of $\tan\beta$, $\text{sgn}(\mu)$. Color code as in Fig. 1. The yellow regions are excluded by ATLAS three leptons plus missing energy search [3].

the large $\tan\beta$ case corresponds to a conservative scenario. As also discussed in section 3 decoupling M_2 yields a conservative bound and thus we set $M_2 = 1$ TeV.

Resulting limits are shown in Fig. 7 projected on the plane of the physical masses $m_{\tilde{\chi}_1^0}$ vs. $m_{\tilde{\chi}_2^0}$. For a lightest neutralino of mass $m_{\tilde{\chi}_1^0} = 35$ GeV, $\tan\beta = 5$ and $\mu > 0$ we find a limit of $m_{\tilde{\chi}_2^0} \lesssim 120$, $m_{\tilde{\chi}_2^0} \gtrsim 260$ GeV. The lower limit is a consequence of the kinematic boundary between on- and off-shell decays at $m_{\tilde{\chi}_2^0} - m_{\tilde{\chi}_1^0} = m_Z$. In the regime of purely off-shell decays of the $\tilde{\chi}_2^0$ various decay modes compete and the ATLAS limit vanishes. Furthermore, as discussed in [21], in this regime branching ratios can still strongly depend on the scale and details of the “decoupled” sfermions, thus conservative exclusion limits are difficult to deduce. For $\tan\beta = 40$ and $\mu < 0$ the upper limits extends up to $m_{\tilde{\chi}_2^0} \gtrsim 280$ GeV. At the same time in this case larger values of $m_{\tilde{\chi}_1^0}$ can be excluded. For all scenarios studied exclusion limits drop sharply at the kinematical threshold $m_{\tilde{\chi}_2^0} - m_{\tilde{\chi}_1^0} = m_h$. In this small corner of the parameter space limits from Wh searches might become relevant [23, 58, 59].

Finally we present the limits of our reinterpretation in the phenomenologically interesting $\tilde{\chi}_1^0$ vs. $|\mu|$ plane, i.e. in the plane where constraints from the thermal relic abundance were discussed in Fig. 1. Results are shown in the upper/lower panel of Fig. 8 for $\tan\beta = 5/40$; on the left and right for $\mu > 0$ and $\mu < 0$ respectively. Regions excluded by LHC searches

are shaded in yellow and as in Fig. 1 regions yielding the correct relic abundance just from neutralino DM are shown in blue, while regions where the abundance of the $\tilde{\chi}_1^0$ could contribute to the overall DM abundance are shown in red. For all choices of $\tan\beta$ and $\text{sgn}(\mu)$ large parts of the Z -resonance regions are excluded. More precisely, at the Z -resonance we find $\mu \gtrsim 250$ GeV, apart from a small strip around $(|\mu| \approx m_{\tilde{\chi}_2^0}) - m_{\tilde{\chi}_1^0} = m_h$ for $\mu > 0$ and in general for very small values of μ (below the $\tilde{\chi}_2^0 \rightarrow Z\tilde{\chi}_1^0$ threshold). However, at least for $\mu > 0$, here the limit from $\text{BR}(h \rightarrow \text{invisible})$ shown in Eq. (20) become relevant, excluding the points shown in grey. Combining these limits for $\tan\beta = 40$ we find

$$m_{\tilde{\chi}_1^0} \gtrsim 40 \text{ GeV} \quad [\mu > 0, \tan\beta = 40]. \quad (29)$$

In the more conservative scenario with $\tan\beta = 5$ the bound is somewhat weaker and we find

$$m_{\tilde{\chi}_1^0} \gtrsim 37 \text{ GeV} \quad [\mu > 0, \tan\beta = 5]. \quad (30)$$

For $\mu < 0$ the constraint from the relic abundance combined with the LEP limit on charginos still yields the strongest bound as very small values of μ cannot be excluded. As we have already seen in section 2.1 here,

$$m_{\tilde{\chi}_1^0} \gtrsim 30 \text{ GeV} \quad [\mu < 0]. \quad (31)$$

Also the h -resonance region can partly be excluded already. Precise limits can be read of Fig. 8. Noteworthy, this region extents to very large values of μ , beyond the scope of even the high energy LHC.

5 Conclusions

In this work, we have studied light neutralino Dark Matter in the MSSM within frameworks where all sfermions are heavy. Interestingly, this feature of the spectrum is shared by both ‘natural SUSY’ and ‘mini split’ scenarios. Under the assumption that the neutralino is a standard thermal relic, CMB measurements of the DM abundance translate into specific requirements the spectrum must fulfill. Since, in our case, sfermions play no role in the computation of the DM relic density, these bounds must be satisfied by the neutralino/chargino sector of the MSSM alone. The generic requirement is that Higgsinos are relatively light, such that the lightest neutralino can couple to Z or h through a non-negligible Higgsino component and thus efficiently annihilate. This condition is strongly relaxed if the neutralino mass approaches the conditions for a resonant enhancement of the annihilation cross section: $m_{\tilde{\chi}_1^0} \simeq m_Z/2$ or $m_{\tilde{\chi}_1^0} \simeq m_h/2$. In such a case, Higgsinos can be as heavy as 450 GeV and 1.2 TeV respectively. This parameter space, depicted in Fig. 1, can be hardly tested by direct and indirect DM search experiments because of a suppression of the relevant cross sections in correspondence of the resonances, as shown in Fig. 3. In contrast, LHC experiments have the potential to partly test our scenario searching for production of Higgsino-like charginos and neutralinos, followed by decays to WZ and the LSP. In fact, the remarkable sensitivity

reached by the LHC experiments in the search for purely electroweakly interacting new particles allows us to directly test the electroweak sector of supersymmetric models without the need of assumptions on the strongly-interacting superpartners.

In section 4, we have presented the results of our reinterpretation of an ATLAS three leptons plus missing energy search. In Fig. 8, we have shown that LHC experiments can set non-trivial constraints on the light neutralino parameter space already with the data collected at $\sqrt{s} = 8$ TeV. In particular, we have seen that the current limit only leaves uncovered the case of a neutralino mass lying close to the resonances (at about 5 GeV or less), as well as the corners of the parameter space corresponding to the kinematical thresholds $|\mu| - m_{\tilde{\chi}_1^0} = m_Z, m_h$, where the three leptons searches lose sensitivity. Combining with further channels, such as di-leptons plus missing energies, as well as searches for Wh events, could further reduce the uncovered corners.

The exercise we have performed demonstrates once more that LHC searches for electroweakly interacting SUSY particles can be successfully interpreted as indirect searches for supersymmetric Dark Matter at collider (especially in combination with the relic density constraints), often resulting in more stringent limits than those set by Dark Matter experiments themselves.

Acknowledgments

We thank Jamie Tattersall for providing us with a private version of **CheckMate**. We would also like to thank Andreas Papaefstathiou for useful discussions and help with **Herwig++**. We also thank Ulrich Ellwanger and Guillaume Drieu La Rochelle for valuable discussions. JML was supported by the European Commission through the ‘‘LHCPhenoNet’’ Initial Training Network PITN-GA-2010-264564. The research of TO is supported by Grants-in-Aid for Scientific Research on Innovative Areas *Unification and Development of the Neutrino Science Frontier* Number 2610 5503.

A Neutralino masses and mixing

The neutralino mass term in the MSSM Lagrangian

$$\mathcal{L} = -\frac{1}{2}(\overline{\psi^c})_\alpha (\mathcal{M}_{\tilde{\chi}^0})_{\alpha\beta} \psi_\beta, \quad (32)$$

is given with the following symmetric matrix,

$$(\mathcal{M}_{\tilde{\chi}^0})_{\alpha\beta} = \begin{pmatrix} M_1 & 0 & -m_Z s_W c_\beta & m_Z s_W s_\beta \\ 0 & M_2 & m_Z c_W c_\beta & -m_Z c_W s_\beta \\ -m_Z s_W c_\beta & m_Z c_W c_\beta & 0 & -\mu \\ m_Z s_W s_\beta & -m_Z c_W s_\beta & -\mu & 0 \end{pmatrix}, \quad (33)$$

in the gauge-interaction basis $\psi_\alpha = (\widetilde{B}, \widetilde{W}^0, \widetilde{H}_d^0, \widetilde{H}_u^0)$, where $s_W = \sin \theta_W$, $c_W = \cos \theta_W$, $s_\beta = \sin \beta$, and $c_\beta = \cos \beta$. Although we diagonalize this mass matrix (with the radiative

corrections) numerically to obtain the mass eigenvalues $m_{\tilde{\chi}_i^0}$ and the mass eigenstates $\tilde{\chi}_i^0 = N_{i\alpha}\psi_\alpha$ with the mixing matrix $N_{i\alpha}$, we derive analytic and approximated expressions to grasp the trend of numerical results.

First, we separate $\mathcal{M}_{\tilde{\chi}^0}$ into the zero-th order part \mathcal{M}_0 and the perturbation $\delta\mathcal{M}$ as $\mathcal{M}_{\tilde{\chi}^0} = \mathcal{M}_0 + \delta\mathcal{M}$. They are defined as

$$(\mathcal{M}_0)_{\alpha\beta} = \begin{pmatrix} M_1 & 0 & 0 & 0 \\ 0 & M_2 & 0 & 0 \\ 0 & 0 & 0 & -\mu \\ 0 & 0 & -\mu & 0 \end{pmatrix}, \quad (34)$$

$$(\delta\mathcal{M})_{\alpha\beta} = \begin{pmatrix} 0 & 0 & -m_Z s_W c_\beta & m_Z s_W s_\beta \\ 0 & 0 & m_Z c_W c_\beta & -m_Z c_W s_\beta \\ -m_Z s_W c_\beta & m_Z c_W c_\beta & 0 & 0 \\ m_Z s_W s_\beta & -m_Z c_W s_\beta & 0 & 0 \end{pmatrix}. \quad (35)$$

The zero-th order part \mathcal{M}_0 can be diagonalized with the zero-th order mixing matrix $N_{i\alpha}^{(0)}$

$$N_{i\alpha}^{(0)} = \begin{pmatrix} 1 & 0 & 0 & 0 \\ 0 & 0 & -\frac{1}{\sqrt{2}} & \frac{1}{\sqrt{2}} \\ 0 & 0 & -\frac{1}{\sqrt{2}} & -\frac{1}{\sqrt{2}} \\ 0 & -1 & 0 & 0 \end{pmatrix}, \quad (36)$$

and the mass eigenvalues at the zero-th order are given as⁵

$$m_{\tilde{\chi}_1^0}^{(0)} = M_1, \quad m_{\tilde{\chi}_2^0}^{(0)} = \mu, \quad m_{\tilde{\chi}_3^0}^{(0)} = -\mu, \quad m_{\tilde{\chi}_4^0}^{(0)} = M_2. \quad (37)$$

Since we assume $M_1 \ll |\mu| \ll M_2$ in our scenario, here we arrange the ordering of the mass eigenstates as described with Eq. (36).

Next, we take into account the effect from the perturbation part $\delta\mathcal{M}$. This perturbation is valid, if the condition $(\delta\mathcal{M})_{ij} \ll |m_{\tilde{\chi}_i^0}^{(0)} - m_{\tilde{\chi}_j^0}^{(0)}|$ is fulfilled, where $(\delta\mathcal{M})_{ij}$ is the perturbation part in the zero-th order mass eigenbasis, i.e., $(\delta\mathcal{M})_{ij} = N_{i\alpha}^{(0)}(\delta\mathcal{M})_{\alpha\beta}N_{\beta j}^{(0)\top}$. In the M_2 decoupling limit, the perturbation terms are proportional to $m_Z s_W$, which is sufficiently smaller than the difference between two mass eigenvalues, which is typically $|\mu|$. After including the first order perturbation, the neutralino mixings $N_{i\alpha}$ result in the followings:

$$N_{i\alpha}^{(0+1)} = \begin{pmatrix} 1 & 0 & \frac{m_Z s_W}{\mu} \left(s_\beta + c_\beta \frac{M_1}{\mu} \right) & -\frac{m_Z s_W}{\mu} \left(c_\beta + s_\beta \frac{M_1}{\mu} \right) \\ \frac{m_Z s_W (s_\beta + c_\beta)}{\sqrt{2}\mu} \left(1 + \frac{M_1}{\mu} \right) & 0 & -\frac{1}{\sqrt{2}} & \frac{1}{\sqrt{2}} \\ \frac{m_Z s_W (s_\beta - c_\beta)}{\sqrt{2}\mu} \left(1 - \frac{M_1}{\mu} \right) & 0 & -\frac{1}{\sqrt{2}} & -\frac{1}{\sqrt{2}} \\ 0 & -1 & 0 & 0 \end{pmatrix}, \quad (38)$$

⁵At the zero-th order, $\tilde{\chi}_2^0$ and $\tilde{\chi}_3^0$ are degenerate in physical mass. The *second lightest* state and the *third lightest* state can be identified only after taking the radiative corrections (and the perturbation) into account. In the case of $\mu > 0$, we identify the state with a mass of μ as a would-be $\tilde{\chi}_2^0$, and that with $-\mu$ as a would-be $\tilde{\chi}_3^0$. In the case of $\mu < 0$, the ordering becomes opposite, i.e., $m_{\tilde{\chi}_2^0}^{(0)} = -\mu(>0)$ and $m_{\tilde{\chi}_3^0}^{(0)} = \mu(<0)$. Therefore, the mixing matrix for the $\mu < 0$ case can be obtained by exchanging $N_{2\alpha}$ and $N_{3\alpha}$ in Eq. (38).

Here, we expand the elements in powers of M_1/μ and leave the terms up to the first order. They fit well with the numerical results evaluated by **SuSpect**. Although the mass eigenvalues do not get the correction at the first order of this perturbation, they are affected by the radiative corrections [65], which are larger than the perturbations. For the analytic expressions of the neutralino masses and mixings in various cases, see e.g., Ref. [66].

References

- [1] G. Aad et al. (ATLAS Collaboration), JHEP **1405**, 071 (2014), 1403.5294.
- [2] V. Khachatryan et al. (CMS Collaboration), Eur.Phys.J. **C74**, 3036 (2014), 1405.7570.
- [3] G. Aad et al. (ATLAS Collaboration), JHEP **1404**, 169 (2014), 1402.7029.
- [4] L. Calibbi, J. M. Lindert, T. Ota, and Y. Takanishi, JHEP **1310**, 132 (2013), 1307.4119.
- [5] L. Calibbi, J. M. Lindert, T. Ota, and Y. Takanishi (2014), 1405.3884.
- [6] A. Arbey, M. Battaglia, and F. Mahmoudi, Phys.Rev. **D88**, 095001 (2013), 1308.2153.
- [7] G. Belanger, G. Drieu La Rochelle, B. Dumont, R. M. Godbole, S. Kraml, et al., Phys.Lett. **B726**, 773 (2013), 1308.3735.
- [8] K. Hagiwara, S. Mukhopadhyay, and J. Nakamura, Phys.Rev. **D89**, 015023 (2014), 1308.6738.
- [9] G. Belanger, S. Biswas, C. Boehm, and B. Mukhopadhyaya, JHEP **12**, 076 (2012), 1206.5404.
- [10] D. Hooper and T. Plehn, Phys. Lett. **B562**, 18 (2003), hep-ph/0212226.
- [11] G. Belanger, F. Boudjema, A. Pukhov, and S. Rosier-Lees (2002), hep-ph/0212227.
- [12] A. Bottino, N. Fornengo, and S. Scopel, Phys. Rev. **D67**, 063519 (2003), hep-ph/0212379.
- [13] H. K. Dreiner et al., Eur. Phys. J. **C62**, 547 (2009), 0901.3485.
- [14] H. K. Dreiner et al., Phys. Rev. **D80**, 035018 (2009), 0905.2051.
- [15] M. Cahill-Rowley, R. Cotta, A. Drlica-Wagner, S. Funk, J. Hewett, et al. (2014), 1405.6716.
- [16] N. Arkani-Hamed, A. Delgado, and G. Giudice, Nucl.Phys. **B741**, 108 (2006), hep-ph/0601041.
- [17] J. Bramante, A. Delgado, F. Elahi, A. Martin, and B. Ostdiek (2014), 1408.6530.

- [18] G. F. Giudice and A. Romanino, Nucl. Phys. **B699**, 65 (2004), [Erratum-ibid.B706:65-89,2005], [hep-ph/0406088](#).
- [19] N. Arkani-Hamed and S. Dimopoulos, JHEP **06**, 073 (2005), [hep-th/0405159](#).
- [20] A. Arvanitaki, N. Craig, S. Dimopoulos, and G. Villadoro (2012), [1210.0555](#).
- [21] A. Bharucha, S. Heinemeyer, and F. von der Pahlen, Eur.Phys.J. **C73**, 2629 (2013), [1307.4237](#).
- [22] S. Gori, S. Jung, and L.-T. Wang, JHEP **1310**, 191 (2013), [1307.5952](#).
- [23] T. Han, S. Padhi, and S. Su, Phys.Rev. **D88**, 115010 (2013), [1309.5966](#).
- [24] P. Schwaller and J. Zurita, JHEP **1403**, 060 (2014), [1312.7350](#).
- [25] Z. Han, G. D. Kribs, A. Martin, and A. Menon, Phys.Rev. **D89**, 075007 (2014), [1401.1235](#).
- [26] C. Han, L. Wu, J. M. Yang, M. Zhang, and Y. Zhang (2014), [1409.4533](#).
- [27] T. A. W. Martin and D. Morrissey (2014), [1409.6322](#).
- [28] T. Nihei, L. Roszkowski, and R. Ruiz de Austri, JHEP **0203**, 031 (2002), [hep-ph/0202009](#).
- [29] H. E. Haber and G. L. Kane, Phys.Rept. **117**, 75 (1985).
- [30] M. Drees and M. M. Nojiri, Phys.Rev. **D47**, 376 (1993), [hep-ph/9207234](#).
- [31] A. Bottino, F. Donato, N. Fornengo, and S. Scopel, Phys.Rev. **D70**, 015005 (2004), [hep-ph/0401186](#).
- [32] A. Bottino, F. Donato, N. Fornengo, and S. Scopel, Phys.Rev. **D78**, 083520 (2008), [0806.4099](#).
- [33] N. Fornengo, S. Scopel, and A. Bottino, Phys.Rev. **D83**, 015001 (2011), [1011.4743](#).
- [34] L. Calibbi, T. Ota, and Y. Takanishi, JHEP **1107**, 013 (2011), [1104.1134](#).
- [35] V. Khachatryan et al. (CMS Collaboration) (2014), [1408.3316](#).
- [36] P. Bechtle, S. Heinemeyer, O. Stal, T. Stefaniak, and G. Weiglein (2014), [1403.1582](#).
- [37] R. Aaij et al. (LHCb Collaboration), Phys.Rev.Lett. **110**, 021801 (2013), [1211.2674](#).
- [38] A. Djouadi, J.-L. Kneur, and G. Moultaka, Comput. Phys. Commun. **176**, 426 (2007), [hep-ph/0211331](#).
- [39] A. Djouadi, M. M. Muhlleitner, and M. Spira, Acta Phys. Polon. **B38**, 635 (2007), [hep-ph/0609292](#).

- [40] G. Belanger, F. Boudjema, A. Pukhov, and A. Semenov, *Comput.Phys.Comm.* **185**, 960 (2014), 1305.0237.
- [41] G. Belanger, F. Boudjema, A. Pukhov, and A. Semenov, *Comput.Phys.Comm.* **176**, 367 (2007), hep-ph/0607059.
- [42] G. Belanger, F. Boudjema, A. Pukhov, and A. Semenov, *Comput.Phys.Comm.* **174**, 577 (2006), hep-ph/0405253.
- [43] G. Belanger, F. Boudjema, A. Pukhov, and A. Semenov, *Comput.Phys.Comm.* **149**, 103 (2002), hep-ph/0112278.
- [44] P. Ade et al. (Planck Collaboration), *Astron.Astrophys.* (2014), 1303.5076.
- [45] J. R. Ellis, J. M. Frere, J. S. Hagelin, G. L. Kane, and S. T. Petcov, *Phys. Lett.* **B132**, 436 (1983).
- [46] A. Bartl, H. Fraas, and W. Majerotto, *Nucl. Phys.* **B278**, 1 (1986).
- [47] R. Barbieri, G. Gamberini, G. F. Giudice, and G. Ridolfi, *Phys. Lett.* **B195**, 500 (1987).
- [48] S. Schael et al. (ALEPH Collaboration, DELPHI Collaboration, L3 Collaboration, OPAL Collaboration, SLD Collaboration, LEP Electroweak Working Group, SLD Electroweak Group, SLD Heavy Flavour Group), *Phys.Rept.* **427**, 257 (2006), hep-ex/0509008.
- [49] P. Bechtle, O. Brein, S. Heinemeyer, G. Weiglein, and K. E. Williams, *Comput. Phys. Commun.* **181**, 138 (2010), 0811.4169.
- [50] P. Bechtle, O. Brein, S. Heinemeyer, G. Weiglein, and K. E. Williams, *Comput. Phys. Commun.* **182**, 2605 (2011), 1102.1898.
- [51] P. Bechtle, O. Brein, S. Heinemeyer, O. Stal, T. Stefaniak, et al., *Eur.Phys.J.* **C74**, 2693 (2014), 1311.0055.
- [52] P. Bechtle, S. Heinemeyer, O. Stal, T. Stefaniak, and G. Weiglein, *Eur.Phys.J.* **C74**, 2711 (2014), 1305.1933.
- [53] K. Griest and H. E. Haber, *Phys. Rev.* **D37**, 719 (1988).
- [54] D. Akerib et al. (LUX Collaboration), *Phys.Rev.Lett.* **112**, 091303 (2014), 1310.8214.
- [55] M. Ackermann et al. (The Fermi-LAT Collaboration), *Phys. Rev. Lett.* **107**, 241302 (2011), URL <http://link.aps.org/doi/10.1103/PhysRevLett.107.241302>.
- [56] C. Han, A. Kobakhidze, N. Liu, A. Saavedra, L. Wu, et al., *JHEP* **1402**, 049 (2014), 1310.4274.
- [57] M. Low and L.-T. Wang, *JHEP* **1408**, 161 (2014), 1404.0682.

- [58] H. Baer, V. Barger, A. Lessa, W. Sreethawong, and X. Tata, Phys.Rev. **D85**, 055022 (2012), 1201.2949.
- [59] A. Papaefstathiou, K. Sakurai, and M. Takeuchi, JHEP **1408**, 176 (2014), 1404.1077.
- [60] W. Beenakker et al., Phys. Rev. Lett. **83**, 3780 (1999), [Erratum-ibid.100:029901,2008], hep-ph/9906298.
- [61] URL <http://hepdata.cedar.ac.uk/view/ins1282905>.
- [62] J. Bellm, S. Gieseke, D. Grellscheid, A. Papaefstathiou, S. Platzer, et al. (2013), 1310.6877.
- [63] M. Drees, H. Dreiner, D. Schmeier, J. Tattersall, and J. S. Kim (2013), 1312.2591.
- [64] J. de Favereau et al. (DELPHES 3), JHEP **1402**, 057 (2014), 1307.6346.
- [65] T. Fritzsche and W. Hollik, Eur.Phys.J. **C24**, 619 (2002), hep-ph/0203159.
- [66] A. Bartl, H. Fraas, W. Majerotto, and N. Oshimo, Phys. Rev. **D40**, 1594 (1989).